ACS OMEGA

Open Access

http://pubs.acs.org/journal/acsodf

Article

Efficient Electrochemical Hydrogenation of Furfural to Furfuryl Alcohol Using an Anion-Exchange Membrane Electrolysis Cell

Sanghwi Han, Yoonjae Lee, Jinse Woo, Junghwan Jang, Yung-Eun Sung, and Jeyong Yoon*

Cite This: *ACS Omega* 2024, 9, 26285−26292

Read Online

ACCESS | Metrics & More | Article Recommendations | Supporting Information

ABSTRACT: The electrochemical hydrogenation (ECH) of furfural (FF) offers a promising pathway for the production of furfuryl alcohol (FA) while aligning with sustainability and environmental considerations. However, this technology has primarily been studied in half-cell configurations operating at high cell voltages and low current densities. Herein, we employ a membrane electrode assembly (MEA) system with an anion-exchange membrane for the ECH of FF and systematically investigate various parameters, including the ionomer content in the cathode catalyst, electrolyte type, electrolyte concentration, and flow rate. Under optimal conditions, our MEA system with non-noble metal-based catalysts exhibits a current density of 30 mA cm^{-2} with a Faradaic efficiency for FA production of 66% at a cell voltage of 2 V, maintaining operational durability for 5 h. This study highlights the potential of electrochemical FA production for practical applications to realize the decarbonization of the hydrogenation industry.

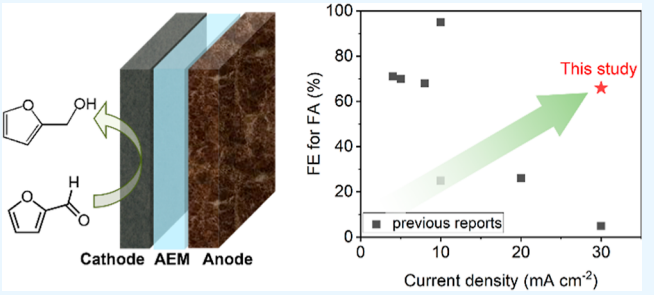

INTRODUCTION

The direct conversion of biomass into valuable chemicals is being intensively pursued to reduce the dependency on petroleum-derived resources amidst the growing environmental and economic concerns.[1−6] Furfural (FF), which is produced from agricultural waste treatment at a commercial scale of 250,000 tons per year,[1,7] stands among the top 12 biomass-derived platform molecules crucial for fuel production.[8] The valorization of FF yields various chemicals, with furfuryl alcohol (FA) as the main derivative accounting for roughly 60% of the FF feedstock due to its extensive demand in the foundry industry for binder production.[1,7,9−12] Conventionally, FA is mainly produced from FF using thermocatalytic hydrogenation methods, exhibiting high selectivity.[13−16] However, these techniques require high temperature (>400 K) and pressure (>5 MPa).[1,12,17,18] Hence, a more sustainable and environmentally friendly approach to upgrading FF into FA is highly desirable.

Electrochemical hydrogenation (ECH) has emerged as an alternative method for converting FF to FA.[19−25] ECH operates under mild conditions without the need for hydrogen gas, utilizing electricity that can be sourced from renewable energy. However, despite its technological potential, the ECH of FF suffers from a series of drawbacks that hinder its practical application. First, most studies on electrochemical FA production predominantly rely on half-cell systems, achieving limited current densities (~20 mA cm^{-2}).[9,10,19,20,23,26−30] Low current densities (~20 mA cm^{-2}) at elevated cell voltages (>2 V) have also been reported in a few studies on FA production using membrane electrode assembly (MEA) cells;[8,31] thus, further understanding and optimization of MEA systems are required. Second, discovering an optimal electrolyte for FA production is imperative to ensure an enhanced selectivity and economic viability. Initially, research on the ECH of FF focused on acidic conditions;[9,11,25,28,32−36] however, acidic electrolytes are prone to side reactions such as hydrogen evolution, 2-methylfuran production, and polymerization and require noble metals such as Pt and Ir for durability.[1,7,17] Therefore, identifying the optimal electrolyte and parameters for the electrochemical production of FA in the MEA systems is crucial.

Herein, we employed a MEA system with an anion-exchange membrane (AEM) for the ECH of FF and systematically investigated various parameters under alkaline conditions. A Cu catalyst was employed as a cathode catalyst due to its exceptional selectivity for FA production,[11,17,19,29] and an electrodeposited FeCo-based catalyst was used as an anode catalyst. Various parameters, including the ionomer content in the Cu catalyst, electrolyte type, electrolyte concentration, and flow rate, were systematically investigated under alkaline conditions, and the optimal conditions in terms of FA production performance and selectivity were identified.

Received: March 4, 2024
Revised: May 27, 2024
Accepted: May 31, 2024
Published: June 7, 2024

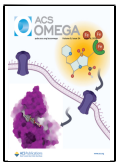

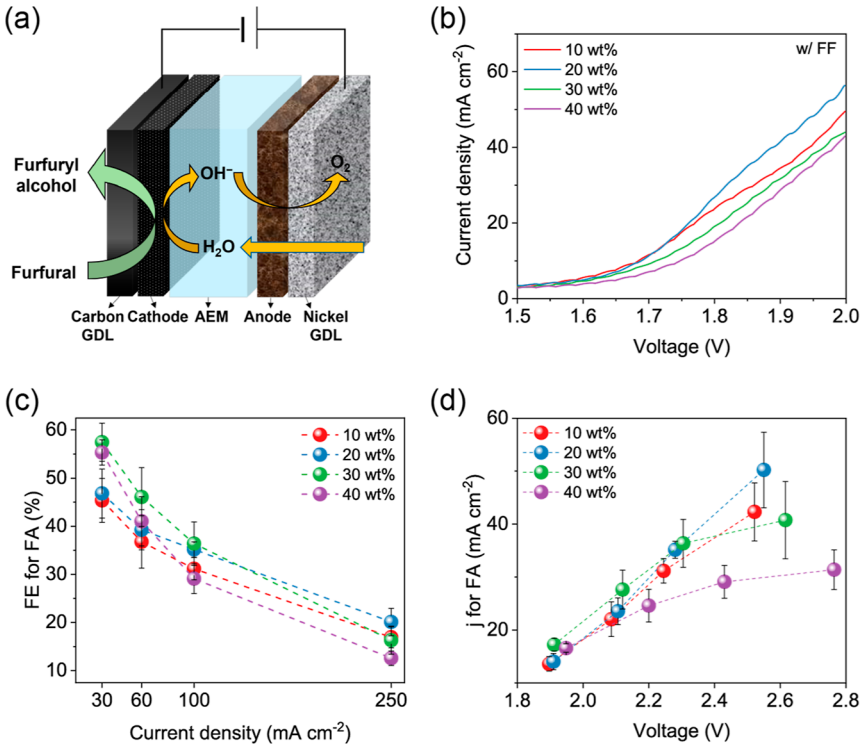

Figure 1. (a) Schematic of the ECH of FF to FA in a MEA system. (b) Polarization curves, (c) FE for FA production, and (d) current density for FA production in the MEA systems with Cu electrodes at varying ionomer contents from 10 to 40 wt % in a solution containing 1 M K_2CO_3 and 0.1 M FF (w/FF).

Under optimum conditions, our system using non-noble-metal-based catalysts attained a current density of 30 mA cm^{-2} at a cell voltage of 2 V with a Faradaic efficiency (FE) of 66%. Moreover, it demonstrated notable durability for 5 h of operation at a constant current density of 30 mA cm^{-2}. These results underscore the promising prospects of electrochemical FA production for practical applications.

EXPERIMENTAL SECTION

Electrocatalyst Preparation. For the cathode catalysts, Cu nanoparticles were prepared via the liquid-phase reduction of $NaBH_4$. First, 0.1 g of carbon black powder was added to 100 mL of deionized water (18.2 MΩ cm, Milli-Q Direct 8 system, Merck Millipore, MA, USA), and the mixture was sonicated for 30 min. Subsequently, $CuCl_2$ (99.9%, Sigma-Aldrich) was added at a concentration of 5 mM, and the mixture was stirred for 1 h. NaOH (98%, Alfa Aesar) was employed to attain a pH of 12, followed by the addition of 10 mL of 0.5 M $NaBH_4$ (99.9%, Sigma-Aldrich). After the solution was stirred for more than 20 h, the Cu nanoparticles were isolated via filtration. The Cu cathode electrode was fabricated by using the spray-coating technique. Briefly, a cathodic ink slurry comprising the synthesized Cu nanoparticles, XB-7 ionomer (Dioxide Materials), water, and isopropyl alcohol, was sonicated for 1 h and then subjected to the spray-coating process, achieving a loading density of 5 mg cm^{-2} on carbon paper (10BC, Sigracet). The ionomer content relative to Cu was adjusted within the range of 10−40 wt %. For the anode catalyst, a FeCo-based catalyst was fabricated via electrodeposition of Fe and Co from a solution containing 25 mM $FeCl_3$ (99.9%, Sigma-Aldrich) and 25 mM of $CoCl_2$ (99.9%, Sigma-Aldrich) on Ni felt (NF, 2Ni18-025, Bekaert) at −0.95 V (vs SCE) for 5 min using a conventional three-electrode electrochemical cell with NF, platinum foil, and a saturated calomel electrode (SCE) as the working, counter, and reference electrodes, respectively.

Electrochemical Evaluation of MEA Systems. The electrochemical assessment of the MEA system was performed using the established AEM water electrolysis single-cell system.[37−39] The single cell consists of a 1 cm^2 Cu cathode, the FeCo-based anode, and an X37-50 grade RT (Dioxide Materials) AEM. Pt-coated Ti flow fields and end plates were provided by the CNL Energy company. A 1 M K_2CO_3 (99.0%, Sigma-Aldrich) solution was supplied to the anode. For the cathode, Li_2CO_3 (99.0%, Sigma-Aldrich), Na_2CO_3 (99.5%, Sigma-Aldrich), or K_2CO_3 solutions were used as electrolytes with and without 0.1 M FF (99.0%, Sigma-Aldrich). All experiments were performed at room temperature. Linear sweep voltammetry (LSV) curves were obtained in the range of 1.0−2.0 V using a scan rate of 10 mV s^{-1}. To ascertain the industrial applicability of FA production, we quantified the FA production amount at high current densities ranging from 30 to 250 mA cm^{-2}. The quantity of FA produced was measured after a constant current density was applied for 3 min. For a durability test, the AEMWE system was operated at 30 mA cm^{-2} for 5 h. Electrochemical impedance spectroscopy (EIS) measurements were conducted at a cell voltage of 1.7 V and an applied amplitude of 10 mV, spanning a frequency range of 10 kHz to 1 Hz.

Product Analysis. The gas and liquid products were quantified via gas chromatography (GC; 7890B, Agilent) and high-performance liquid chromatography (HPLC; YL9100 HPLC system, YL Instrument), respectively, which are generally used to analyze both FF and FA.[9,19,40,41] For the analysis of the gas products, the cathode compartment of the flow cell was linked to a GC, directing the exit stream from the

https://doi.org/10.1021/acsomega.4c02107
ACS Omega 2024, 9, 26285−26292

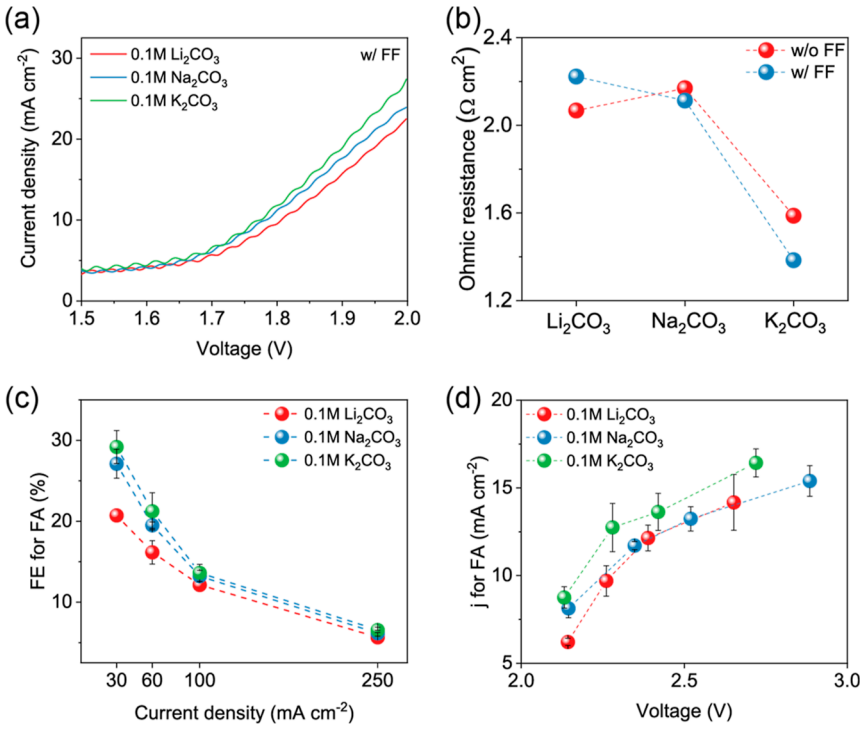

Figure 2. (a) LSV curves, (b) ohmic resistance, (c) FE for FA production, and (d) current density for FA production in MEA systems with solutions containing 0.1 M FF with 0.1 M Li_2CO_3, Na_2CO_3, or K_2CO_3.

ECH cell into the gas sampling loop of the GC. The gas products in the exit stream were analyzed by using a thermal conductivity detector. For the analysis of the liquid products, samples from the cathode reservoir were collected, 10-fold-diluted with acetonitrile (ACN; HPLC grade, 99.8+%, Thermo Scientific), and subsequently analyzed via HPLC. A mixture of ACN and DI in a ratio of 2:8 was employed as the eluent, and the resulting product was quantified by using a UV detector at 220 nm. Quantitative analysis was conducted through external calibration using standards at FF and FA concentrations ranging from 0.05 to 10 mM. The quantities of products obtained from the GC and HPLC analyses were employed to determine the FE of products according to eq 1

$$\text{FE}\ (\%) = \frac{n \times F \times m}{Q} \times 100 \quad (1)$$

where n represents the number of electrons involved in the ECH to produce one molecule, F is the Faraday constant (96,485 C mol^{-1}), m represents the amount of produced products in moles, and Q represents the total charge passed.

Materials Characterization. Surface morphology was evaluated via scanning electron microscopy (SEM) analysis using a JSM-7800F Prime microscope (JEOL, Japan) operating at 15 kV, conducted at the National Center for Inter-university Research Facilities (NCIRF) located at Seoul National University (SNU). X-ray photoelectron spectroscopy (XPS) analysis was conducted utilizing a K-alpha system (Thermo Fisher Scientific, UK) incorporating an Al Kα μ-focused monochromator operating at 1486.6 eV. The crystal structure was analyzed using X-ray diffraction (XRD) with a SmartLab system (Rigaku, Japan) employing Cu Kα radiation (40 kV, 250 mA) within the 2θ range of 30−80°, at a scan speed of 4° s^{-1}.

RESULTS AND DISCUSSION

Figure 1 depicts a schematic of the MEA system for electrochemical FA generation and shows the influence of the ionomer content in the Cu cathode on the FA production performance. In our MEA system, FA is produced via the reaction between FF and water at the cathode, and produced OH^- migrates toward the anode across the AEM to generate O_2 (Figure 1a). A 1 M K_2CO_3 solution was employed in the anode, and a mixed solution containing 1 M K_2CO_3 and 0.1 M FF was used in the cathode. To explore whether ionomers play a comparable role in FA production systems as they do in water electrolysis, we conducted experiments varying ionomer content in the 1 M K_2CO_3 electrolytes with (w/FF) and without FF (w/o FF). Figure 1b illustrates the LSV curves of the MEA systems using Cu catalysts at varying ionomer contents ranging from 10 to 40 wt %. Among these systems, the MEA system with the Cu catalyst containing 20 wt % ionomer exhibited the highest current density of approximately 60 mA cm^{-2} at a cell voltage of 2 V. Even in the absence of FF, the MEA system with the Cu catalyst containing 20 wt % of ionomer displayed superior performance to other systems (Figure S1). The FA produced at current densities of 30, 60, 100, and 250 mA cm^{-2} was quantified via HPLC (Figure S2), and the FE was calculated (Figure 1c). At 30 mA cm^{-2}, the Cu system comprising 30 wt % of ionomer exhibited the highest FE of ∼58%. However, at 250 mA cm^{-2}, the Cu system with an ionomer content of 20 wt % showed the highest FE of approximately 22%. For a comprehensive comparison of the performance and FE for FA production, the current density for FA versus cell voltage plots of each system is shown in Figure 1d. Each cell voltage represents the stabilized value obtained during the continuous operation under a constant current density. At around 1.9 V, all systems demonstrated similar current densities, while the system with the Cu catalyst

https://doi.org/10.1021/acsomega.4c02107
ACS Omega 2024, 9, 26285−26292

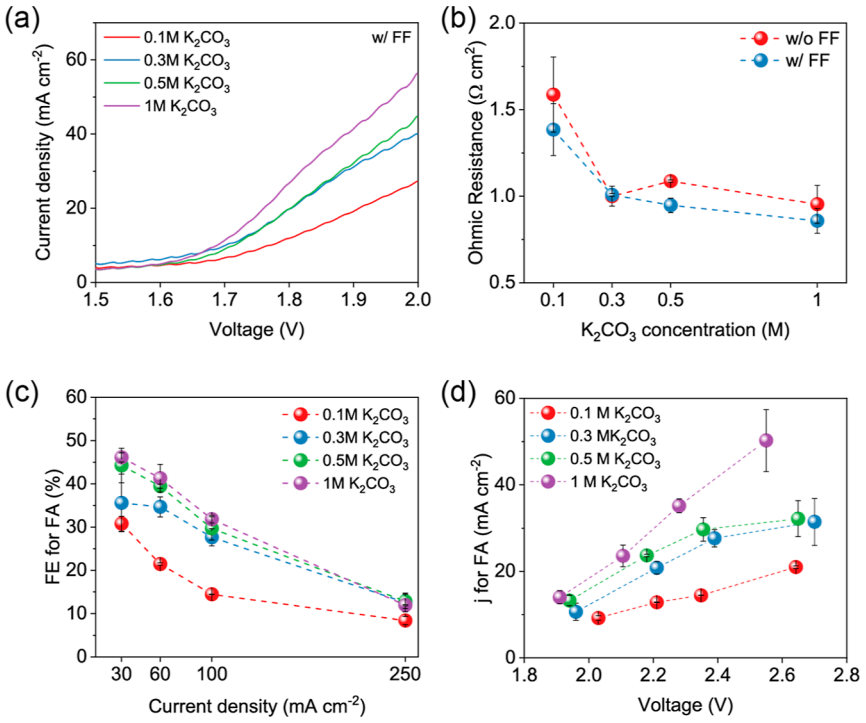

Figure 3. Comparison of (a) polarization curves, (b) ohmic resistance, (c) FE for FA production, and (d) current density for FA production in MEA systems with varying K_2CO_3 concentrations in the 0.1 M FF solution.

containing 20 wt % of ionomer showcased superior performance, delivering a current density of ∼50 mA cm^{-2} at approximately 2.5 V. Given that the performance trend based on ionomer content remains consistent regardless of the presence or absence of FF, it is posited that the observed trend, wherein optimal ionomer content enhances ion conduction and mass transfer in water electrolysis,[42−46] is also applicable to the ECH of FF. Accordingly, an ionomer concentration of 20 wt % was selected as the optimal condition for the subsequent experiments.

Next, the effect of the cation in the cathode electrolyte on the FA production performance was investigated by comparing 0.1 M Li_2CO_3, Na_2CO_3, and K_2CO_3 solutions (Figure 2). To minimize pH effects, the pH of all solutions was controlled at 12. Figure 2a shows that the MEA system with K_2CO_3 afforded the highest performance among others, exhibiting ∼27 mA cm^{-2} at 2 V. This trend, which was observed even in the absence of FF (Figure S3a), can be attributed to the lower ohmic resistance of the system with K_2CO_3 compared with other electrolytes (Figures 2b and S3b,c). In addition, the MEA system with a K_2CO_3 electrolyte exhibited the highest FE for FA among all of the systems at all current densities (Figure 2c). Among the electrolytes, Li_2CO_3 exhibited the lowest FE for FA. At all cell voltage ranges, the K_2CO_3 electrolyte consistently provided superior performance in terms of the current density for FA production (Figure 2d). These results demonstrate the pronounced influence of the cations in electrolytes on both the performance and selectivity for FA production. As established in the field of CO_2 reduction, this phenomenon can be attributed to the fact that with increasing cation size, the pK_a of cations diminished, and thereby the buffering capacity decreases in the order $K^+ > Na^+ > Li^+$, which resulted in diminishing the HER.[47,48] Consequently, K_2CO_3 was selected as the optimal electrolyte for electrochemical FA production in the MEA system.

Alkaline electrolytes can avoid the use of noble metal catalysts and reduce side reactions like hydrogen evolution, 2-methylfuran production, and polymerization but may also induce the Cannizzaro reaction.[17,22,49−51] Thus, identifying the optimal molarity and pH for alkaline electrolytes is essential to minimize side reactions and ensure a high FA production performance. Figure 3 illustrates the FA production performance depending on the K_2CO_3 concentration at a constant FF concentration of 0.1 M. To mitigate the Cannizzaro reaction, which occurs at high pH and was confirmed even in 0.1 M KOH with 0.1 M FF in our experiments, we adjusted the pH to 12 for the K_2CO_3 electrolyte test. Figure 3a shows an obvious performance increase with increasing K_2CO_3 concentration irrespective of the presence of FF (Figure S4a). As observed in the LSV results, an increase in the K_2CO_3 concentration resulted in a decrease in the ohmic resistance of the system (Figures 3b and S4b,c). Notably, the electrolyte composed of 1 M K_2CO_3 and 0.1 M FF demonstrated the lowest ohmic resistance of 0.9 Ω cm^2. Furthermore, the MEA system with this electrolyte exhibited superior FE for FA production compared to other systems at all current density ranges (Figure 3c) and consistently demonstrated the highest FA production performance at all measured cell voltage ranges (Figure 3d). Given the observed correlation between the electrolyte concentration and FA production performance, electrolytes with higher concentrations of either K_2CO_3 or FF were also investigated. Three solutions, i.e., 1 M K_2CO_3 + 0.1 M FF, 1 M K_2CO_3 + 0.2 M FF, and 2 M K_2CO_3 + 0.1 M FF, were prepared and evaluated as electrolytes to determine the occurrence of spontaneous side reactions. Initially, all the three electrolytes exhibited a light brown color, which was retained for the 1 M K_2CO_3 + 0.1 M FF electrolyte after 20 h, whereas the 1 M K_2CO_3 + 0.2 M FF and 2 M K_2CO_3 + 0.1 M FF electrolytes turned darker (Figure S5a). This can be attributed to polymer formation via the Cannizzaro reaction.[17,22,49−51]

https://doi.org/10.1021/acsomega.4c02107
ACS Omega 2024, 9, 26285−26292

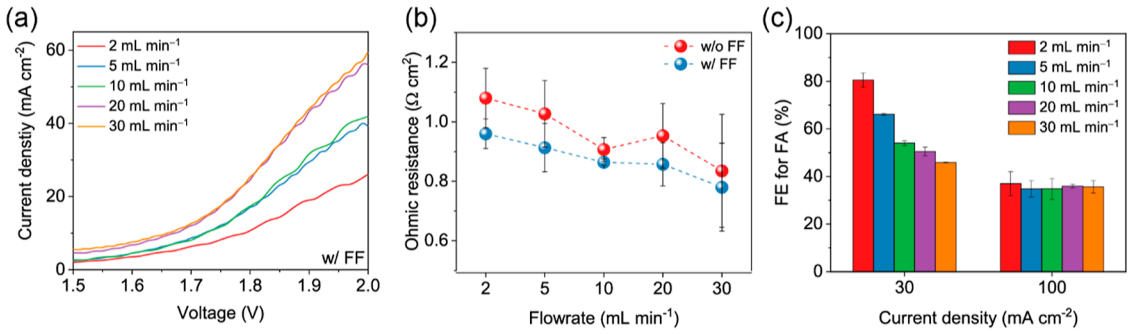

Figure 4. Comparison of (a) polarization curves, (b) ohmic resistance, and (c) FE for FA in MEA systems with varying flow rates from 2 to 30 mL min^{-1} in a solution containing 1 M K_2CO_3 and 0.1 M FF.

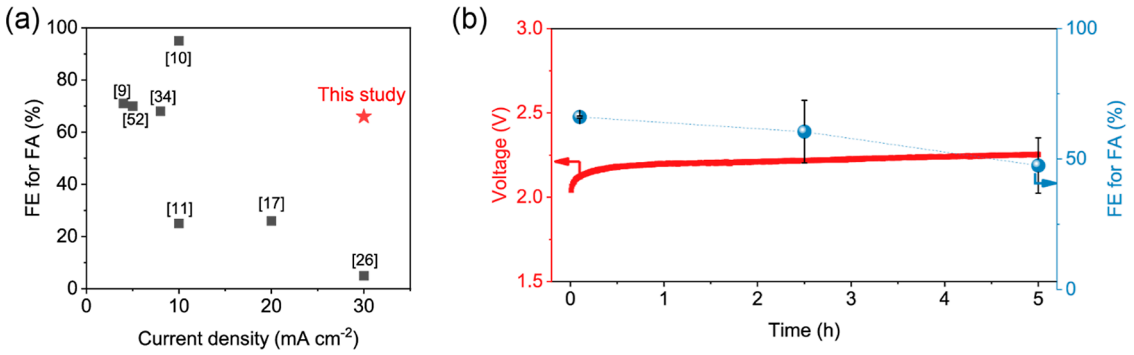

Figure 5. (a) Comparison of the performance of the Cu-based MEA system with previous state-of-the-art FF hydrogenation catalysts.[9−11,17,26,34,52] (b) Cell voltage and FE profiles for the ECH of FF to FA of the optimized MEA system at 30 mA cm^{-2} for 5 h. Conditions: Cu cathode with an ionomer content of 20 wt %, 5 mL min^{-1} of flow rate, and 1 M K_2CO_3 + 0.1 M FF solution.

To quantify the byproducts resulting from the Cannizzaro reaction, the products were measured over time. Due to the difficulties in polymer quantification via HPLC, the comparison primarily focused on FA production. For all electrolytes, FA was not detected within the first hour of the reaction. However, after 3 h, approximately 0.06 mM FA was produced in the 1 M K_2CO_3 + 0.2 M FF and 2 M K_2CO_3 + 0.1 M FF electrolytes but not in the 1 M K_2CO_3 + 0.1 M FF electrolyte (Figure S5b). After 20 h, approximately 0.2 mM FA was generated in the 1 M K_2CO_3 + 0.2 M FF and 2 M K_2CO_3 + 0.1 M FF electrolytes, while nearly half that amount was produced in the 1 M K_2CO_3 + 0.1 M FF electrolyte. These results demonstrate that excess K_2CO_3 or FF induces side reactions, such as the Cannizzaro reaction, highlighting the importance of controlling the pH and molarity of the electrolyte. Therefore, we selected the 1 M K_2CO_3 + 0.1 M FF solution as the optimal electrolyte composition and employed it in subsequent experiments.

Figure 4 shows the relationship between the FA production performance and the flow rate. The flow rate significantly influences mass transfer, thereby affecting both FA production rate and selectivity. Flow rates of 2, 5, 10, 20, and 30 mL min^{-1} were evaluated using the 1 M K_2CO_3 + 0.1 M FF electrolyte. The current densities of the systems at 2 V were improved with increasing flow rates and then stabilized at approximately 60 mA cm^{-2} after reaching a plateau beyond a flow rate of 20 mL min^{-1} (Figure 4a). The limited performance at lower flow rates stemmed from an insufficient reactant supply to the catalyst layer.[43] In this setup, a flow rate of around 20 mL min^{-1} provided an adequate reactant supply. Along with the performance trend, a reduction in ohmic resistance irrespective of the presence of FF occurred with an increasing flow rate (Figures 4b and S6). However, at a current density of 30 mA cm^{-2}, a noticeable increase in the FE for FA production was observed as the flow rate decreased (Figure 4c). At a flow rate of 2 mL min^{-1}, the MEA system displayed ∼80% FE for FA at 30 mA cm^{-2}, representing the highest FE among the systems. However, this correlation was not verified at 100 mA cm^{-2}, where the FE remained consistently around 38% across all flow rates. Because FF inhibits the adsorption of the proton source at the catalyst surface, lower flow rates may impede the access of the proton source to the catalyst surface, enhancing the selectivity for FA production by inhibiting the HER. However, at high current densities, the depletion of FF on the catalyst surface enables water access, leading to diminished FE for FA regardless of flow rate. Considering both high performance and selectivity for FA production, a flow rate of 5 mL min^{-1} was selected as the optimal condition, and the product analysis via HPLC and GC confirmed the exclusive presence of H_2 and FA (Figure S7). Under the optimal conditions, our system demonstrated superior FE for FA production at a relatively high current density, outperforming state-of-the-art catalysts (Figure 5a and Table 1).[9−11,17,26,34,52] Moreover, in contrast with the majority of studies, which were conducted using half-cell systems requiring high cell voltages, our system exhibited a high performance at a cell voltage of approximately 2 V. We also compared our system with conventional thermocatalytic hydrogenation technologies, showing FA selectivity comparable to previous research under ambient conditions of temperature and pressure (Table S1).[13−16] To assess the economic viability of ECH of FF for the FA production process, a techno-economic analysis (TEA) was conducted based on the previous studies (see details in the Supporting Information).[53−55] Based on the TEA using our experimental

https://doi.org/10.1021/acsomega.4c02107
ACS Omega 2024, 9, 26285−26292

Table 1. Comparison of the Performance of the Cu-Based MEA System with Reported FF Hydrogenation Systems[9−11,17,26,34,52]

catalyst	FA selectivity (%)	current density (mA cm^{-2})	references
Cu	**66**	**30**	**this study**
Cu	25	10	11
Cu	71	4	9
Cu/Cu-400 nm	5	30	20
AgPd	95	10	10
Cu_1/PC	70	5	52
Cu/NC900	26	20	17
$CuPd_{0.012}$/C	68	8	34

results, FA production via the ECH method with the MEA system ($1076 per ton of FA) showed higher economic efficiency than conventional methods ($1347 per ton of FA). This finding indicates the potential economic viability of the electrochemical FA production method, albeit necessitating further research on scale-up and enhancement of system performance and durability.

The optimized MEA system could be operated continuously at 30 mA cm^{-2} for 5 h with an increase of approximately 0.2 V in the cell voltage, maintaining a FE of around 50% (Figure 5b). Our system demonstrates notable durability compared with previous reports describing shorter durability (~3 h) at low current densities (~15 mA cm^{-2}).[8,17,26,31] After the durability test, the ohmic resistance of the system increased by approximately 1.1 Ω cm^2, which can be attributed to membrane degradation or inadequate catalyst contact (Figure S8). To assess catalyst properties pre- and postdurability testing, XPS and SEM analyses were conducted. In the Cu 2p spectra, the peak around 932.5 eV indicates Cu^0/Cu^+, and the peak at approximately 933.8 eV corresponds to Cu^{2+} (Figure S9a).[56] For O 1sp spectra, O_L (lattice oxygen, ~529.7 eV) and O═C (~532.2 eV) peaks were shown (Figure S9c).[57] Initially, the Cu electrode exhibited dominance of the Cu^{2+} peak, yet postdurability testing, the prevalence shifts toward the Cu^0/Cu^+ peak. Furthermore, following the durability test, the initially observed O_L peak was no longer observable. This result can be due to the electrochemical reduction of the Cu catalyst within the reducing atmosphere for FA formation. XRD analysis also revealed the transformation of the Cu catalyst from CuO to Cu/Cu_2O following the durability test (Figure S10). SEM analysis indicates that the Cu catalyst comprises nanoparticles on the order of tens of nanometers, with insignificant surface changes observed before and after the durability test (Figure S11). Overall, this study highlights the decent performance and durability of FA production in MEA systems using non-noble metal-based catalysts, demonstrating their potential for practical FA production. To enhance the FA production performance and durability in this MEA system, further research into catalyst and membrane development is required.

CONCLUSIONS

In conclusion, our extensive exploration of parameters for the ECH of FF employing a MEA system under alkaline conditions resulted in a notable FA production performance. A series of parameters, including the Cu catalyst ionomer content, electrolyte type, electrolyte concentration, and flow rate, were investigated, and the optimal condition in terms of FA production performance and selectivity was identified. Under the optimal condition, our system achieved a current density of 30 mA cm^{-2} with a FE of 66% for FA production at a cell voltage of 2 V. Furthermore, it exhibited remarkable durability during 5 h operation at a constant current density of 30 mA cm^{-2}. This study underscores the potential of electrochemical FA production for practical application, supporting the decarbonization of the hydrogenation industry.

ASSOCIATED CONTENT

Supporting Information

The Supporting Information is available free of charge at https://pubs.acs.org/doi/10.1021/acsomega.4c02107.

HPLC data; LSV and EIS plots in parametric MEA systems; FA production data according to electrolyte composition; Faraday efficiency for FA and H_2 during electrolysis; TEA analysis; EIS plots of the optimized MEA system at initial and after 5 h of operation; and XPS and SEM data for Cu electrodes (PDF)

AUTHOR INFORMATION

Corresponding Author

Jeyong Yoon − *School of Chemical and Biological Engineering, Institute of Chemical Processes, Seoul National University (SNU), Seoul 08826, Republic of Korea;* orcid.org/0000-0003-4455-3670; Email: jeyong@snu.ac.kr

Authors

Sanghwi Han − *School of Chemical and Biological Engineering, Institute of Chemical Processes, Seoul National University (SNU), Seoul 08826, Republic of Korea;* orcid.org/0000-0002-0017-1550

Yoonjae Lee − *School of Chemical and Biological Engineering, Institute of Chemical Processes, Seoul National University (SNU), Seoul 08826, Republic of Korea*

Jinse Woo − *School of Chemical and Biological Engineering, Institute of Chemical Processes, Seoul National University (SNU), Seoul 08826, Republic of Korea;* orcid.org/0009-0002-4340-784X

Junghwan Jang − *Center for Nanoparticle Research, Institute for Basic Science (IBS), Seoul 08826, Republic of Korea; School of Chemical and Biological Engineering, Institute of Chemical Processes, Seoul National University (SNU), Seoul 08826, Republic of Korea*

Yung-Eun Sung − *Center for Nanoparticle Research, Institute for Basic Science (IBS), Seoul 08826, Republic of Korea; School of Chemical and Biological Engineering, Institute of Chemical Processes, Seoul National University (SNU), Seoul 08826, Republic of Korea;* orcid.org/0000-0002-1563-8328

Complete contact information is available at: https://pubs.acs.org/10.1021/acsomega.4c02107

Notes

The authors declare no competing financial interest.

ACKNOWLEDGMENTS

This paper was based on the results obtained from projects, NRF-2022R1A2C109193 and NRF-2018R1A5A1024127, commissioned by the National Research Foundation of Korea. This work was also supported by Project Code IBS-R006-A2 from the Institute for Basic Science (IBS).

REFERENCES

(1) Dixit, R. J.; Bhattacharyya, K.; Ramani, V. K.; Basu, S. Electrocatalytic Hydrogenation of Furfural Using Non-Noble-Metal Electrocatalysts in Alkaline Medium. *Green Chem.* **2021**, *23* (11), 4201−4212.

(2) Kwon, Y.; Schouten, K. J. P.; Van Der Waal, J. C.; De Jong, E.; Koper, M. T. M. Electrocatalytic Conversion of Furanic Compounds. *ACS Catal.* **2016**, *6* (10), 6704−6717.

(3) Han, S.; Jeon, S.-i.; Lee, J.; Ahn, J.; Lee, C.; Lee, J.; Yoon, J. Efficient Bicarbonate Removal and Recovery of Ammonium Bicarbonate as CO2 Utilization Using Flow-Electrode Capacitive Deionization. *Chem. Eng. J.* **2022**, *431*, 134233.

(4) Jiang, H.; Wu, X.; Zhang, H.; Yan, Q.; Li, H.; Ma, T.; Yang, S. Toward Effective Electrocatalytic C-N Coupling for the Synthesis of Organic Nitrogenous Compounds Using CO 2 and Biomass as Carbon Sources. *SusMat* **2023**, *3* (6), 781−820.

(5) Yan, Q.; Wu, X.; Jiang, H.; Wang, H.; Xu, F.; Li, H.; Zhang, H.; Yang, S. Transition Metals-Catalyzed Amination of Biomass Feedstocks for Sustainable Construction of N-Heterocycles. *Coord. Chem. Rev.* **2024**, *502*, 215622.

(6) He, L.; Chen, L.; Zheng, B.; Zhou, H.; Wang, H.; Li, H.; Zhang, H.; Xu, C. C.; Yang, S. Deep Eutectic Solvents for Catalytic Biodiesel Production from Liquid Biomass and Upgrading of Solid Biomass into 5-Hydroxymethylfurfural. *Green Chem.* **2023**, *25* (19), 7410−7440.

(7) May, A. S.; Biddinger, E. J. Strategies to Control Electrochemical Hydrogenation and Hydrogenolysis of Furfural and Minimize Undesired Side Reactions. *ACS Catal.* **2020**, *10* (5), 3212−3221.

(8) Diaz, L. A.; Lister, T. E.; Rae, C.; Wood, N. D. Anion Exchange Membrane Electrolyzers as Alternative for Upgrading of Biomass-Derived Molecules. *ACS Sustain. Chem. Eng.* **2018**, *6* (7), 8458−8467.

(9) Liu, L.; Liu, H.; Huang, W.; He, Y.; Zhang, W.; Wang, C.; Lin, H. Mechanism and Kinetics of the Electrocatalytic Hydrogenation of Furfural to Furfuryl Alcohol. *J. Electroanal. Chem.* **2017**, *804*, 248−253.

(10) Brosnahan, J. T.; Zhang, Z.; Yin, Z.; Zhang, S. Electrocatalytic Reduction of Furfural with High Selectivity to Furfuryl Alcohol Using AgPd Alloy Nanoparticles. *Nanoscale* **2021**, *13* (4), 2312−2316.

(11) Jung, S.; Biddinger, E. J. Electrocatalytic Hydrogenation and Hydrogenolysis of Furfural and the Impact of Homogeneous Side Reactions of Furanic Compounds in Acidic Electrolytes. *ACS Sustain. Chem. Eng.* **2016**, *4* (12), 6500−6508.

(12) An, Z.; Li, J. Recent Advances in the Catalytic Transfer Hydrogenation of Furfural to Furfuryl Alcohol over Heterogeneous Catalysts. *Green Chem.* **2022**, *24* (5), 1780−1808.

(13) Yan, K.; Chen, A. Efficient Hydrogenation of Biomass-Derived Furfural and Levulinic Acid on the Facilely Synthesized Noble-Metal-Free Cu-Cr Catalyst. *Energy* **2013**, *58*, 357−363.

(14) Lee, J.; Seo, J. H.; Nguyen-Huy, C.; Yang, E.; Lee, J. G.; Lee, H.; Jang, E. J.; Kwak, J. H.; Lee, J. H.; Lee, H.; An, K. Cu2O(100) Surface as an Active Site for Catalytic Furfural Hydrogenation. *Appl. Catal., B* **2021**, *282*, 119576.

(15) Lee, J. G.; Yoon, S.; Yang, E.; Lee, J. H.; Song, K.; Moon, H. R.; An, K. Structural Evolution of ZIF-67-Derived Catalysts for Furfural Hydrogenation. *J. Catal.* **2020**, *392*, 302−312.

(16) Islam, M. J.; Granollers Mesa, M.; Osatiashtiani, A.; Taylor, M. J.; Manayil, J. C.; Parlett, C. M. A.; Isaacs, M. A.; Kyriakou, G. The Effect of Metal Precursor on Copper Phase Dispersion and Nanoparticle Formation for the Catalytic Transformations of Furfural. *Appl. Catal., B* **2020**, *273*, 119062.

(17) Xu, W.; Yu, C.; Chen, J.; Liu, Z. Electrochemical Hydrogenation of Biomass-Based Furfural in Aqueous Media by Cu Catalyst Supported on N-Doped Hierarchically Porous Carbon. *Appl. Catal., B* **2022**, *305*, 121062.

(18) Yu, I. K. M. Mechanistic Understanding of the Catalytic Hydrogenation of Bio-Derived Aromatics. *Green Chem.* **2021**, *23* (23), 9239−9253.

(19) Parpot, P.; Bettencourt, A. P.; Chamoulaud, G.; Kokoh, K. B.; Belgsir, E. M. Electrochemical investigations of the oxidation−reduction of furfural in aqueous medium. *Electrochim. Acta* **2004**, *49* (3), 397−403.

(20) Nilges, P.; Schröder, U. Electrochemistry for Biofuel Generation: Production of Furans by Electrocatalytic Hydrogenation of Furfurals. *Energy Environ. Sci.* **2013**, *6* (10), 2925−2931.

(21) Shan, N.; Hanchett, M. K.; Liu, B. Mechanistic Insights Evaluating Ag, Pb, and Ni as Electrocatalysts for Furfural Reduction from First-Principles Methods. *J. Phys. Chem. C* **2017**, *121* (46), 25768−25777.

(22) Carneiro, J.; Nikolla, E. Electrochemical Conversion of Biomass-Based Oxygenated Compounds. *Annu. Rev. Chem. Biomol. Eng.* **2019**, *10*, 85−104.

(23) Lenk, T.; Rabet, S.; Sprick, M.; Raabe, G.; Schröder, U. Insight into the Interaction of Furfural with Metallic Surfaces in the Electrochemical Hydrogenation Process. *ChemPhysChem* **2023**, *24* (5), No. e202200614.

(24) Mukadam, Z.; Liu, S.; Pedersen, A.; Barrio, J.; Fearn, S.; Sarma, S. C.; Titirici, M. M.; Scott, S. B.; Stephens, I. E. L.; Chan, K.; Mezzavilla, S. Furfural Electrovalorisation Using Single-Atom Molecular Catalysts. *Energy Environ. Sci.* **2023**, *16*, 2934−2944.

(25) Delima, R. S.; Stankovic, M. D.; Macleod, B. P.; Fink, A. G.; Rooney, M. B.; Huang, A.; Jansonius, R. P.; Dvorak, D. J.; Berlinguette, C. P. Selective Hydrogenation of Furfural Using a Membrane Reactor. *Energy Environ. Sci.* **2022**, *15* (1), 215−224.

(26) Jung, S.; Karaiskakis, A. N.; Biddinger, E. J. Enhanced Activity for Electrochemical Hydrogenation and Hydrogenolysis of Furfural to Biofuel Using Electrodeposited Cu Catalysts. *Catal. Today* **2019**, *323*, 26−34.

(27) Fang, W.; Liu, S.; Steffensen, A. K.; Schill, L.; Kastlunger, G.; Riisager, A. On the Role of Cu + and CuNi Alloy Phases in Mesoporous CuNi Catalyst for Furfural Hydrogenation. *ACS Catal.* **2023**, *13*, 8437−8444.

(28) Ketkaew, M.; Assavapanumat, S.; Klinyod, S.; Kuhn, A.; Wattanakit, C. Bifunctional Pt/Au Janus Electrocatalysts for Simultaneous Oxidation/Reduction of Furfural with Bipolar Electrochemistry. *Chem. Commun.* **2022**, *58* (27), 4312−4315.

(29) Xia, Z.; Li, Y.; Wu, J.; Huang, Y. C.; Zhao, W.; Lu, Y.; Pan, Y.; Yue, X.; Wang, Y.; Dong, C. L.; Wang, S.; Zou, Y. Promoting the Electrochemical Hydrogenation of Furfural by Synergistic Cu0-Cu+ Active Sites. *Sci. China: Chem.* **2022**, *65* (12), 2588−2595.

(30) Bharath, G.; Banat, F. High-Grade Biofuel Synthesis from Paired Electrohydrogenation and Electrooxidation of Furfural Using Symmetric Ru/Reduced Graphene Oxide Electrodes. *ACS Appl. Mater. Interfaces* **2021**, *13*, 24643−24653.

(31) Cao, Y.; Noël, T. Efficient Electrocatalytic Reduction of Furfural to Furfuryl Alcohol in a Microchannel Flow Reactor. *Org. Process Res. Dev.* **2019**, *23* (3), 403−408.

(32) May, A. S.; Biddinger, E. J. Modeling Competing Kinetics between Electrochemical Reduction of Furfural on Copper and Homogeneous Side Reactions in Acid. *Energy Fuels* **2022**, *36* (18), 11001−11011.

(33) May, A. S.; Watt, S. M.; Biddinger, E. J. Kinetics of Furfural Electrochemical Hydrogenation and Hydrogenolysis in Acidic Media on Copper. *React. Chem. Eng.* **2021**, *6* (11), 2075−2086.

(34) Zhou, P.; Li, L.; Mosali, V. S. S.; Chen, Y.; Luan, P.; Gu, Q.; Turner, D. R.; Huang, L.; Zhang, J. Electrochemical Hydrogenation of Furfural in Aqueous Acetic Acid Media with Enhanced 2-Methylfuran Selectivity Using CuPd Bimetallic Catalysts. *Angew. Chem., Int. Ed.* **2022**, *61* (13), No. e202117809.

(35) Jung, S.; Biddinger, E. J. Controlling Competitive Side Reactions in the Electrochemical Upgrading of Furfural to Biofuel. *Energy Technol.* **2018**, *6* (7), 1370−1379.

(36) Chadderdon, X. H.; Chadderdon, D. J.; Matthiesen, J. E.; Qiu, Y.; Carraher, J. M.; Tessonnier, J. P.; Li, W. Mechanisms of Furfural Reduction on Metal Electrodes: Distinguishing Pathways for Selective Hydrogenation of Bioderived Oxygenates. *J. Am. Chem. Soc.* **2017**, *139* (40), 14120−14128.

https://doi.org/10.1021/acsomega.4c02107
ACS Omega 2024, 9, 26285−26292

(37) Han, S.; Park, J.; Yoon, J. Surface Reconstruction of Co-Based Catalysts for Enhanced Oxygen Evolution Activity in Anion Exchange Membrane Water Electrolysis. *Adv. Funct. Mater.* **2024**, *34*, 2314573.
(38) Han, S.; Park, H. S.; Yoon, J. Superior Performance of an Anion Exchange Membrane Water Electrolyzer: Sequential Electrodeposited Co-Based Oxygen Evolution Catalyst. *Chem. Eng. J.* **2023**, *477*, 146713.
(39) Han, S.; Ryu, J. H.; Lee, W. B.; Ryu, J.; Yoon, J. Translating the Optimized Durability of Co-Based Anode Catalyst into Sustainable Anion Exchange Membrane Water Electrolysis. *Small* **2024**, 2311052.
(40) Li, J.; Xu, Y.; Zhang, M.; Wang, D. Determination of Furfural and 5-Hydroxymethylfurfural in Biomass Hydrolysate by High-Performance Liquid Chromatography. *Energy Fuels* **2017**, *31* (12), 13769−13774.
(41) Zhou, L.; Li, Y.; Lu, Y.; Wang, S.; Zou, Y. PH-Induced Selective Electrocatalytic Hydrogenation of Furfural on Cu Electrodes. *Chin. J. Catal.* **2022**, *43* (12), 3142−3153.
(42) Cho, M. K.; Park, H. Y.; Choe, S.; Yoo, S. J.; Kim, J. Y.; Kim, H. J.; Henkensmeier, D.; Lee, S. Y.; Sung, Y. E.; Park, H. S.; Jang, J. H. Factors in Electrode Fabrication for Performance Enhancement of Anion Exchange Membrane Water Electrolysis. *J. Power Sources* **2017**, *347*, 283−290.
(43) Park, J. E.; Kang, S. Y.; Oh, S. H.; Kim, J. K.; Lim, M. S.; Ahn, C. Y.; Cho, Y. H.; Sung, Y. E. High-Performance Anion-Exchange Membrane Water Electrolysis. *Electrochim. Acta* **2019**, *295*, 99−106.
(44) Lim, A.; Kim, H.-j.; Henkensmeier, D.; Jong Yoo, S.; Young Kim, J.; Young Lee, S.; Sung, Y. E.; Jang, J. H.; Park, H. S. A Study on Electrode Fabrication and Operation Variables Affecting the Performance of Anion Exchange Membrane Water Electrolysis. *J. Ind. Eng. Chem.* **2019**, *76*, 410−418.
(45) Cho, M. K.; Park, H. Y.; Lee, H. J.; Kim, H. J.; Lim, A.; Henkensmeier, D.; Yoo, S. J.; Kim, J. Y.; Lee, S. Y.; Park, H. S.; Jang, J. H. Alkaline Anion Exchange Membrane Water Electrolysis: Effects of Electrolyte Feed Method and Electrode Binder Content. *J. Power Sources* **2018**, *382*, 22−29.
(46) Li, D.; Park, E. J.; Zhu, W.; Shi, Q.; Zhou, Y.; Tian, H.; Lin, Y.; Serov, A.; Zulevi, B.; Baca, E. D.; Fujimoto, C.; Chung, H. T.; Kim, Y. S. Highly Quaternized Polystyrene Ionomers for High Performance Anion Exchange Membrane Water Electrolysers. *Nat. Energy* **2020**, *5* (5), 378−385.
(47) Yu, J.; Xiao, J.; Ma, Y.; Zhou, J.; Lu, P.; Wang, K.; Yan, Y.; Zeng, J.; Wang, Y.; Song, S.; Fan, Z. Acidic Conditions for Efficient Carbon Dioxide Electroreduction in Flow and MEA Cells. *Chem Catal.* **2023**, *3* (8), 100670.
(48) Zhang, T.; Zhou, J.; Luo, T.; Lu, J. Q.; Li, Z.; Weng, X.; Yang, F. Acidic CO2 Electrolysis Addressing the "Alkalinity Issue" and Achieving High CO2 Utilization. *Chem.—Eur. J.* **2023**, *29* (46), No. e202301455.
(49) Liu, H.; Patel, D. M.; Chen, Y.; Lee, J.; Lee, T. H.; Cady, S. D.; Cochran, E. W.; Roling, L. T.; Li, W. Unraveling Electroreductive Mechanisms of Biomass-Derived Aldehydes via Tailoring Interfacial Environments. *ACS Catal.* **2022**, *12* (22), 14072−14085.
(50) Liu, H.; Agrawal, N.; Ganguly, A.; Chen, Y.; Lee, J.; Yu, J.; Huang, W.; Mba Wright, M.; Janik, M. J.; Li, W. Ultra-Low Voltage Bipolar Hydrogen Production from Biomass-Derived Aldehydes and Water in Membrane-Less Electrolyzers. *Energy Environ. Sci.* **2022**, *15* (10), 4175−4189.
(51) Li, X.; Cong, L.; Wu, Y.; Lin, N.; Liu, F.; Xin, D.; Han, F.; Yang, J.; Chen, W.; Lin, H. Strategies for Controlling Gas Evolution Reactions to Boost the Divergent Paired Electrochemical Upgrading of Furfural in Acidic Environment. *Chem. Eng. J.* **2023**, *470*, 144093.
(52) Zhou, P.; Chen, Y.; Luan, P.; Zhang, X.; Yuan, Z.; Guo, S. X.; Gu, Q.; Johannessen, B.; Mollah, M.; Chaffee, A. L.; Turner, D. R.; Zhang, J. Selective Electrochemical Hydrogenation of Furfural to 2-Methylfuran over a Single Atom Cu Catalyst under Mild PH Conditions. *Green Chem.* **2021**, *23* (8), 3028−3038.
(53) Viar, N.; Agirre, I.; Gandarias, I. Process Design, Kinetics, and Techno-Economic Assessment of an Integrated Liquid Phase Furfural Hydrogenation Process. *Chem. Eng. J.* **2024**, *480*, 147873.
(54) Lv, X. H.; Huang, H.; Cui, L. T.; Zhou, Z. Y.; Wu, W.; Wang, Y. C.; Sun, S. G. Hydrogen Spillover Accelerates Electrocatalytic Semi-Hydrogenation of Acetylene in Membrane Electrode Assembly Reactor. *ACS Appl. Mater. Interfaces* **2024**, *16* (7), 8668−8678.
(55) Zhao, B. H.; Chen, F.; Wang, M.; Cheng, C.; Wu, Y.; Liu, C.; Yu, Y.; Zhang, B. Economically Viable Electrocatalytic Ethylene Production with High Yield and Selectivity. *Nat. Sustain.* **2023**, *6* (7), 827−837.
(56) Biesinger, M. C. Advanced Analysis of Copper X-Ray Photoelectron Spectra. *Surf. Interface Anal.* **2017**, *49* (13), 1325−1334.
(57) Sivaranjini, B.; Mangaiyarkarasi, R.; Ganesh, V.; Umadevi, S. Vertical Alignment of Liquid Crystals over a Functionalized Flexible Substrate. *Sci. Rep.* **2018**, *8* (1), 8891.

https://doi.org/10.1021/acsomega.4c02107
ACS Omega 2024, 9, 26285−26292